

Abstract

Persistent jet structures along zonal and meridional fields, believed to be caused by stationary gravity waves, were detected in February 1999 in MST wind measurements of the troposphere and lower stratosphere over Jicamarca, Peru. Over a seven day span, two days of observations showed signatures of a Doppler ducted gravity wave in the upper troposphere/lower stratosphere. Herein we present the observations, their characteristics, and results of numerical simulations used to mimic these observed features. Though a fair replication of the observed ducted structure in the numerical model is found, the observed period of ~ 90 min is nonetheless longer than anticipated and raises concern as to the specific physical nature of the observed structures. However, given the high quality of the observations, we demonstrate that continued analysis of this data set and concurrent modeling will allow for a better understanding of Doppler ducts at high spatial and temporal resolution which can ultimately be applied to studies of mesospheric ducts and bores.

1 Introduction

The observed behavior of mesospheric fronts, primarily in all-sky imagery utilizing mesospheric emissions of O, OH, and Na, presents a challenge to our understanding of the dynamics of the mesosphere-lower thermosphere (MLT) region. The first observation of a mesospheric frontal structure, i.e., a phenomenon characterized by an intense wave front followed by a series of training crests and propagating in the MLT, was reported in Taylor et al. (1995). Based on these observations, and inspired by the similarity between such airglow disturbance events and undular tidal bores in rivers, Dewan and Picard (1998) and Dewan and Picard (2001) proposed a semi-quantitative model of such a phenomena and coined the term: “mesospheric bore”. The physical basis of these structures is still a matter of investigation (Brown et al., 2004); therefore we shall refer to such observations as “mesospheric fronts”. Smith et al. (2003) reported

Lower stratospheric doppler ducted gravity waves

Z. Li et al.

Title Page

Abstract

Introduction

Conclusions

References

Tables

Figures



Back

Close

Full Screen / Esc

Printer-friendly Version

Interactive Discussion



observing a mesospheric front that traveled at the same altitude over 1200 kilometers without significant dissipation – thus representing a unique process of mesoscale energy transport in the middle atmosphere. Snively and Pasko (2003), Snively et al. (2007), and Snively and Pasko (2008) showed that the appearance of a mesospheric front was much like the signature of a ducted gravity wave, albeit missing an intense leading band. Brown et al. (2004) showed that such mesospheric fronts were associated with passing tropospheric weather fronts, likely generating gravity waves which propagated upwards and then were sustained by thermal ducts within mesospheric inversion layers (MILs) (Meriwether and Gerrard, 2004). This idea is supported by the observations of She et al. (2004) using concurrent measurements of winds and temperatures from Na lidar. Recently, Fehine et al. (2009) reported the observation of a mesospheric front in a Doppler duct (Chimonas and Hines, 1986) during the 1 October 2005 SpreadFEx campaign in South America.

To date, there is considerable uncertainty in the realms of (a) what mechanisms sustain mesospheric fronts (the role of thermal ducts and Doppler ducts, both separately and together), (b) how a mesospheric front propagates (whether as bores (Dewan and Picard, 1998) or as ducted gravity waves (Snively et al., 2007) or as something else), (c) the potential impact of such phenomena on the MLT region in particular, and (d) mechanisms that lead to the creation of a mesospheric front. Progress in these areas is hampered by the fact that mesospheric fronts are very difficult to study due to the experimental challenges associated with measurements of fundamental base-state parameters of the MLT region, let alone the acquisition of synoptic-state of the MLT. Even high-resolution modeling efforts are challenging due to the myriad of physics occurring over dramatically different temporal and spatial scales.

In an effort to better answer these questions, we have turned to high resolution upper tropospheric/lower stratospheric wind observations made with the mesosphere-stratosphere-troposphere (MST) radar over Jicamarca, Peru (12° S, 77° W). Inspection of data from February 1999 time-period shows consistently (temporally) steady, sustained winds in the zonal and meridional directions that spatially vary in the vertical.

**Lower stratospheric
doppler ducted
gravity waves**

Z. Li et al.

[Title Page](#)[Abstract](#)[Introduction](#)[Conclusions](#)[References](#)[Tables](#)[Figures](#)[Back](#)[Close](#)[Full Screen / Esc](#)[Printer-friendly Version](#)[Interactive Discussion](#)

**Lower stratospheric
doppler ducted
gravity waves**

Z. Li et al.

Title Page

Abstract

Introduction

Conclusions

References

Tables

Figures

◀

▶

◀

▶

Back

Close

Full Screen / Esc

Printer-friendly Version

Interactive Discussion



The structure of these winds is indicative of stationary gravity wave structure; likely the result of climatological southeasterly or northwesterly tropospheric flow over the terrain generating sustained topographically generated gravity waves (as seen in Fig. 1). Thus, it was suspected that these wind fields would form a natural laboratory for the high resolution study of any Doppler-ducted gravity waves and bore-like phenomena, likely generated by non-stationary or quasi-stationary sources such as tropical convection.

In this paper, analysis of wave structures observed over Jicamarca – which resemble Doppler-ducted gravity waves – are presented. Features found in the data prompted us to numerically simulate the ducting of a traveling gravity wave and investigate if the model results can match the observations. Based on this analysis, we suggest that similar, additional measurements of MST winds over Jicamarca can be incorporated in our model to better understand Doppler-ducted mesospheric fronts.

2 Observations

Prior MST observations (e.g., Woodman and Guillen (1974)) utilizing the Jicamarca incoherent scatter radar observations above the Jicamarca incoherent scatter radar are presented and discussed in Riggini et al. (2002) and Riggini et al. (2004). The 50-MHz radar is divided into four separate antennas pointing at a 2.5° zenith angle in the cardinal directions. Coherent backscatter caused by irregularities in the atmospheric refractive index are collected by each antenna in the radial direction, and the first moment of each spectra is used to determine the radial Doppler shift. The raw data are then post-processed yielding reduced zonal and meridional wind data in 2 min temporal realizations and 150 m range bins. Range-time plots of samples of these data, taken on days 57 and 59 of February 1999, are shown in Fig. 2 (left column). It is important to note that the signal-to-noise ratio varies with altitude due to shifts in the backscattered power; with the highest SNR values being measured in the 1–12 km and the 17–21 km regions. This does not imply that data outside of these regions are poor, but rather that

they are relatively more noisy.

Also shown in Fig. 2 (right column) are the daily mean zonal and meridional winds for the two sample days presented here. A fifth-order polynomial was fitted to the daily mean vertical wind profile and then subtracted from each of the individual measurements – the residue being the wind perturbations. These wind perturbations were then low-pass filtered with filter cutoffs of 1 h and 1.5 km in the time and range domains, respectively, for display purposes only. The resultant low-pass filtered wind perturbations are also shown in Fig. 2 (center column).

Detailed analysis of 7 consecutive days of Jicamarca MST data from February 1999 shows four notable features. First, the winds are consistently steady over the course of multiple days, with deviations being short-lived (<1 h) and comparatively weak (<5 m/s, with respect to the daily mean profile). Over the course of 3–4 consecutive days, the westerly and easterly wind jets/bands would slowly vary with altitude, but showed no coherent phase progression.

Second, vertical wind profiles of both the zonal and meridional winds across the upper troposphere and lower stratosphere indicate a steady background wind superposed with a sinusoidal variation; particularly above 10 km. Removal of the daily mean wind shows perturbations (i.e., Fig. 2, center column) that look like stationary gravity wave structure (i.e., fixed phase structure in time). Assuming that these gravity waves are stationary given their characteristic described earlier, the dispersion relationship for gravity waves is used to infer the horizontal wavelength. On day 59, for instance, the dominantly zonal and easterly horizontal wind speed between 15 and 23 km altitude is estimated to be ~ 10 m/s, with vertical wavelength of ~ 7 km. Utilizing a climatological Brunt-Vaisala frequency, one can show that the horizontal wavelength is ~ 8 km. For day 57, the zonal background wind is weaker than the mean, with an estimated value of ~ 7 m/s and vertical wavelength is much smaller at an estimated ~ 4 km, thus yielding an estimated horizontal wavelength of ~ 9 km. If the horizontal wind profiles were constant with height, these horizontal wavelengths would approximately match the dominant spatial modulation of the ground terrain of ~ 12 km, found from spectral analysis of the

**Lower stratospheric
doppler ducted
gravity waves**

Z. Li et al.

Title Page

Abstract

Introduction

Conclusions

References

Tables

Figures



Back

Close

Full Screen / Esc

Printer-friendly Version

Interactive Discussion



topography shown in Fig. 1, but the change in the background wind velocity with height likely leads to refraction of such gravity waves leading to modifications in the horizontal structure. Nonetheless, we see comparable horizontal wavelength values on not only these two days, but on most days in February.

5 Third, on two of the studied February days (Fig. 2, days 57 and day 59) there appears to be a ductal feature consisting of alternating vertical bands with a periodicity, similar in form to that shown in the modeling results of Snively and Pasko (2003) (i.e., alternating vertical bands with a periodicity of order 10 min). Data from other days in February, even on consecutive days like day 58, did not demonstrate the pattern. The ducting structure is seen in the zonal, meridional, and vertical wind profiles, on both
10 days around 15:00 LT at approximately 15 km altitude. On day 57, the zonal variations are seen in the lowest altitude westward wind excursion from the otherwise easterly wind profile, which corresponds to a northward wind excursion in the meridional wind profile. On day 59, the zonal variations are seen in the lowest altitude eastward wind excursion from the otherwise easterly wind profile, which corresponds to a southward wind excursion in the meridional wind profile; opposite that observed on day 57.

In Fig. 3 we show a closeup of the ductal feature seen in the afternoon on day 57, without any filtering, though we note that ducting signatures were also seen earlier in the day. The observed ducted waves in the westerly jet at 16 km altitude have an
20 observed (residual) horizontal amplitude between 3–5 m/s and an observed period of ~90 min. An estimate of the zonal (and meridional and vertical, not shown) wind power spectral density indicate that the feature is not monochromatic (although there is a local peak in the PSD at approximately 72 min) and instead resembles the PSD of a “square wave,” indicating potential amplitude saturation or mode mixing. Any apparent propagation direction and speed could not be determined. These results are consistent
25 with analysis done with data on day 59, but at 14 km altitude.

Fourth, on day 57, there even appears to be a traveling, upward propagating gravity wave (i.e., downward tilted phase line progression) occurring at approximately 11:00 LT and ending around 16:00 LT, with a vertical wavelength of ~6 km and an observed

**Lower stratospheric
doppler ducted
gravity waves**

Z. Li et al.

Title Page

Abstract

Introduction

Conclusions

References

Tables

Figures

◀

▶

◀

▶

Back

Close

Full Screen / Esc

Printer-friendly Version

Interactive Discussion



period of ~ 4 h. No similar traveling wave signatures were seen on the other days.

3 Numerical model

Combining the features seen in the second and third set of observations, we propose that the observations constitute a Doppler-ducted gravity wave, sustained by the steady easterly or westerly phases of the zonal and meridional wind profiles. To explore this idea further, we have developed a time-stepped two-dimensional (spatial x-horizontal and z-vertical domains) numerical model similar to Snively and Pasko (2003), to examine the conditions in the upper troposphere/lower stratosphere that would allow the occurrence of such a ducting event. The model structure follows the frame work for implementing high-resolution Godunov-type methods (LeVeque, 2003), and is implemented within the CLAWPACK software package (<http://www.amath.washington.edu/~claw>).

The model is similar to the one by Ahmad and Lindeman (2007), which assumes that the atmosphere is represented by an ideal, dry, inviscid gas. The basic governing equations for atmospheric flows are given by conservation of mass, momentum, energy and equation of state, which can be simplified to the following 2D Euler equations:

$$\frac{\partial U}{\partial t} + \frac{\partial F}{\partial x} + \frac{\partial G}{\partial y} = Q \quad (1)$$

with

$$U = \begin{bmatrix} \rho \\ \rho u \\ \rho v \\ \rho \theta \end{bmatrix} \quad F = \begin{bmatrix} \rho u \\ \rho u^2 + p \\ \rho uv \\ \rho u \theta \end{bmatrix}$$
$$G = \begin{bmatrix} \rho v \\ \rho uv \\ \rho v^2 + p \\ \rho v \theta \end{bmatrix} \quad Q = \begin{bmatrix} 0 \\ 0 \\ -\rho g + F_s \\ 0 \end{bmatrix}$$

19017

Lower stratospheric doppler ducted gravity waves

Z. Li et al.

Title Page

Abstract

Introduction

Conclusions

References

Tables

Figures

◀

▶

◀

▶

Back

Close

Full Screen / Esc

Printer-friendly Version

Interactive Discussion



Lower stratospheric doppler ducted gravity waves

Z. Li et al.

Title Page

Abstract

Introduction

Conclusions

References

Tables

Figures

◀

▶

◀

▶

Back

Close

Full Screen / Esc

Printer-friendly Version

Interactive Discussion



where ρ is the atmosphere density, u is the horizontal velocity along the x-direction, v is the vertical velocity along the z-direction, p is the pressure, θ is the potential temperature, and F is a forcing function in the vertical (Andrews et al., 1987). This set of equations is hyperbolic in nature and we adapt a Godunov-type scheme for hyperbolic conservation laws suggested by LeVeque (2003), employing flux-based wave decompositions proposed by Ahmad and Lindeman (2007) to solve the Riemann problems.

The uppermost height of domain simulation is chosen to be 220 km with a sponge layer spanning from 200 km to 220 km. The sponge is thus at a much higher than the altitude that we are interested in modeling; such a configuration was selected to maximally reduce gravity wave reflection from the top model layer and therefore ensure an open boundary condition for the simulation. The horizontal extent of the numerical domain is 1200 km with a 100 km thick sponge layer at both sides –again for open boundary considerations. The vertical and horizontal model resolutions are 0.25 km and 1 km, respectively, and the nominal time-step is chosen to satisfy the Courant parameter. Model output was recorded every 5 s.

The atmospheric background state parameters were specified at the beginning of the run and not allowed to vary in time. An isothermal background temperature was used in this simulation, with $T = 300$ K (and correctly converted to potential temperature, θ). Such a temperature background removes any potential for thermal ducting, thus allowing us to focus on only Doppler ducting. For this simulation we have run the model with two different zonal wind profiles. The first was a windless run that serves as a control run. The second wind profile was also windless, except for Gaussian-shaped jet of maximum amplitude of -15 m/s, centroid altitude of 15 km, $1-\sigma$ vertical width of 4 km, and which filled the horizontal domain, based on the wind observations shown in Fig. 2.

In order to spawn a potentially ducted wave, a source disturbance is used in the model that mimics the effects of a localized vertical oscillation with a characteristic horizontal wavelength $\frac{2\pi}{kx}$, frequency ω , and amplitude modulated by a Gaussian envelope

in space and time ($\sigma_t, \sigma_x, \sigma_z$). The source took the mathematical form of

$$F_s(x, z, t) = F_0 \exp\left(-\frac{(x-x_0)^2}{2\sigma_x^2} - \frac{(z-z_0)^2}{2\sigma_z^2} - \frac{(t-t_0)^2}{2\sigma_t^2}\right) \cos(k_x x) \cos(\omega t) \quad (2)$$

and was located at x_0 and z_0 of 450 km and 3 km, respectively. The horizontal, vertical, and temporal scales of the disturbance were 10 km, 2 km, and 5.86 min (approximately the Brunt-Vaisala frequency), respectively. The initial amplitude disturbance was equivalent to a 1.2 cm/s vertical wind, and the horizontal wavelength and period were initially set to 20 km and 10 min, respectively.

Results of the two model runs are shown in Fig. 4. For the control run (right column) we model an upwards propagating gravity that extends well into the upper atmosphere. There is no indication of any ducting structures. For the run with a westward, Gaussian-shaped jet centered at 15 km (left column), we clearly see ducted waves of 85.4 % of the initial source at time 16 000 s, an observed horizontal wavelength of ~ 20 km, and propagation to the east with an observed speed of ~ 15 m/s. We note that the peaks have an amplitude that is modulated by a broad Gaussian envelope, much like the observations, which is imposed by the source term expression. A change of this source term expression can likewise modulate the peak amplitudes.

If observed from a fixed site, the simulated ducted structure would have a period of ~ 22 min – approximately a fourth as much as the period of the ductal-feature observed over Jicamarca. In an effort to match the observed period, we undertook a number of modeling runs that used various configurations of the above parameters. Generally, we saw that changing the model source parameters (i.e., the horizontal wavenumber and period by factors of up to 3) did not dramatically alter the observed period of the ducted wave. However, changing the width of the wind jet did modify the ductal structure, with a narrower duct resulting in a slower progressing wave packet and thus a longer observed wave period. A wind jet with a RMS width of 1 km resulted in a ducted feature that had an observed period of 90 min. We are still investigating this nature of the duct width and the period that a sustained wave would have, as explored theoretically in

**Lower stratospheric
doppler ducted
gravity waves**

Z. Li et al.

Title Page

Abstract

Introduction

Conclusions

References

Tables

Figures



Back

Close

Full Screen / Esc

Printer-friendly Version

Interactive Discussion



4 Discussion and conclusions

Based on our modeling analysis, when a traveling gravity wave impinges on a spatially confined wind jet (i.e., a Doppler duct), Doppler-mode ducting of the gravity wave is observed in our numerical model. Comparison of the model output with the Jicamarca observations provides evidence that we are observing the signature of a Doppler-ducted gravity wave within the sinusoidal wind variations of the upper troposphere/lower stratosphere.

While the model results do replicate the observations quite well, there are nonetheless important aspects of the observations that need to be resolved. The first issue deals with resolving the meteorology of the upper troposphere/lower stratosphere above Jicamarca. A better determination needs to be made as to whether the vertically-varying sinusoidal variations in the background wind are indeed due to stationary gravity waves, or long-period Kelvin waves, or perhaps due to convective rolls. Given the topology of the terrain surrounding Jicamarca, we have assumed that it was a stationary gravity wave but further studies and reverse gravity wave ray-tracing are needed to confirm this.

The second issue deals with identifying the source of the observed Doppler-ducted gravity waves. Data from day 57 indicate a traveling gravity wave may have “seeded” the duct, but no such traveling gravity wave signature was present on day 59. Furthermore, seeing that the ducted structure was observed at approximately the same time of day for both observations presented here, there may be a diurnal heating mechanism responsible for the ducted wave “seeding.”

The third and most important issue deals with the broader question of whether or not a Doppler-ducted feature was really observed. That is, the spatially confined periodicities could well be the result of a more complex phenomena, like wave breaking due to dynamical instabilities. This issue is beyond the scope of this work at this time but

Lower stratospheric doppler ducted gravity waves

Z. Li et al.

Title Page

Abstract

Introduction

Conclusions

References

Tables

Figures

◀

▶

◀

▶

Back

Close

Full Screen / Esc

Printer-friendly Version

Interactive Discussion



certainly needs to be considered, especially considering that this initial study involved the use of a limited data sample from the larger MST data set. Further studies are required to study this extensive dataset and better characterize the occurrences of these features.

5 Should these three issues be satisfactorily resolved, the upper troposphere/lower stratosphere environment above a location such as Jicamarca would be an ideal natural laboratory to study Doppler ducting phenomena, including gravity wave ducting and potential “bore” formation in Doppler ducts. The steady winds provide excellent dynamical ducts for extended periods of time and the equatorial location provides a plethora
10 of convective gravity wave sources. Furthermore, the excellent signal-to-noise ratio from the Jicamarca MST system, combined with radiosonde data and meteorological diagnostics, would allow for a detailed study of the physics of ducting, including duct-coupling and “kissing modes.” These unique factors should motivate further modeling efforts and observations.

15 *Acknowledgements.* The authors would like to thank Ronald Woodman for both taking this data set and for his constructive comments. We also thank the personnel of the Radio Observatorio de Jicamarca for their assistance in collecting and preparing this data set. We very much appreciate the helpful comments of the reviewers of this paper. This work was supported by grants from the National Science Foundation (NSF-ATM-0735452 and NSF-ATM-0457277).

20 References

- Ahmad, N. and Lindeman, J.: Euler solutions using flux-based wave decomposition, *Int. J. Num. Meth. Fluid.*, 54, C72, 2007. 19017, 19018
- Andrews, D. G., Holton, J. R., and Leovy, C. B.: *Middle Atmosphere Dynamics*, Academic Press, New York, USA, 175–187, 1987. 19018
- 25 Brown, L. B., Gerrard, A. J., Meriwether, J. W., and Makela, J. J.: All-sky imaging observations of mesospheric fronts in OI 557.7 nm and broadband OH airglow emissions: Analysis of frontal structure, atmospheric background conditions, and potential sourcing mechanisms, *J. Geophys. Res.*, 109, D19104, doi:10.1029/2003JD004223, 2004. 19012, 19013

Lower stratospheric doppler ducted gravity waves

Z. Li et al.

Title Page

Abstract

Introduction

Conclusions

References

Tables

Figures



Back

Close

Full Screen / Esc

Printer-friendly Version

Interactive Discussion



- Chimonas, G. and C. O. Hines: Doppler Ducting of Atmospheric Gravity Waves, *J. Geophys. Res.*, 91, 1219–1230, 1986. 19013, 19020
- Dewan, E. M. and Picard, R. H.: Mesospheric bores, *J. Geophys. Res.* 103, 6295–6306, 1998. 19012, 19013
- 5 Dewan, E. M. and Picard, R. H.: On the origin of mesospheric bores, *J. Geophys. Res.*, 106, C2927, doi:10.1029/2000JD900697, 2001 19012
- Fechine, J., Wrasse, C. M., Takahashi, H., Medeiros, A. F., Batista, P. P., Clemesha, B. R., Lima, L. M., Fritts, D., Laughman, B., Taylor, M. J., Pautet, P. D., Mlynczak, M. G., and Russell, J. M.: First observation of an undular mesospheric bore in a Doppler duct, *Ann. Geophys.* 27, 1399–1406, doi:10.5194/angeo-27-1399-2009, 2009. 19013
- 10 LeVeque, R. J.: Clawpack version 4.2 user's guide, Technical Report, University of Washington, USA, <http://www.amath.washington.edu/claw>, 2003. 19017, 19018
- Meriwether, J. W. and Gerrard, A. J.: Mesosphere inversion layers and stratosphere temperature enhancements, *Rev. Geophys.*, 42, RG3003, doi:10.1029/2003RG000133, 2004. 19013
- 15 Riggins, D. M., Kudeki, E., Feng, Z., Sarango, M. F. and Lieberman, R. S.: Jicamarca radar observations of the diurnal and semidiurnal tide in the troposphere and lower stratosphere. *J. Geophys. Res.*, 107, 4062, doi:10.129/2001JD001216, 2002. 19014
- Riggins, D. M., Kudeki, E., and Sarango, M.: Tropospheric and stratospheric momentum flux measurements from radar wind data collected at Jicamarca, *J. Atmos. Solar-Terr. Phys.*, 66, 277–283, 2004. 19014
- 20 She, C. Y., Li, T., Williams, B. P., Yuan, T., and Picard, R. H.: Concurrent OH imager and sodium temperature/wind lidar observation of a mesopause region undular bore event over Fort Collins/Platteville, Colorado, *J. Geophys. Res.* 109, 22107–22115, 2004. 19013
- Snively, J. B. and Pasko, V. P.: Breaking of thunderstorm-generated gravity waves as a source of short-period ducted waves at mesopause altitudes, *Geophys. Res. Lett.*, 30(24), 2254, doi:10.1029/2003GL018436, 2003. 19013, 19016, 19017
- 25 Snively, J. B., Pasko, V. P., Taylor, M. J., and Hocking, W. K.: Doppler ducting of short period gravity waves by mid-latitude tidal wind structure, *J. Geophys. Res.* 112, A03304, doi:10.1029/2006JA011895, 2007. 19013
- 30 Snively, J. B. and Pasko, V. P.: Excitation of Mesospheric Gravity Waves by Tropospheric Sources, *J. Geophys. Res.* 113, A06303, doi:10.1029/2007JA012693, 2008. 19013
- Smith, S. M., Taylor, M. J., Swenson, G. R., She, C. Y., Hocking, W., Baumgardner, J., and Mendillo, M.: A multidagnostic investigation of the mesospheric bore phenomenon *J. Geo-*

**Lower stratospheric
doppler ducted
gravity waves**

Z. Li et al.

Title Page

Abstract

Introduction

Conclusions

References

Tables

Figures

◀

▶

◀

▶

Back

Close

Full Screen / Esc

Printer-friendly Version

Interactive Discussion



phys. Res. 108, 1083–1101, 2003. 19012
Taylor, M. J., Turnbull, D. N., and Lowe, R. P.: Spectrometric and imaging measurements of a spectacular gravity wave event observed during the ALOHA-93 campaign, Geophys. Res. Lett. 20, 2849–2852, 1995. 19012

19023

ACPD

11, 19011–19027, 2011

**Lower stratospheric
doppler ducted
gravity waves**

Z. Li et al.

Title Page

Abstract

Introduction

Conclusions

References

Tables

Figures



Back

Close

Full Screen / Esc

Printer-friendly Version

Interactive Discussion



Lower stratospheric doppler ducted gravity waves

Z. Li et al.

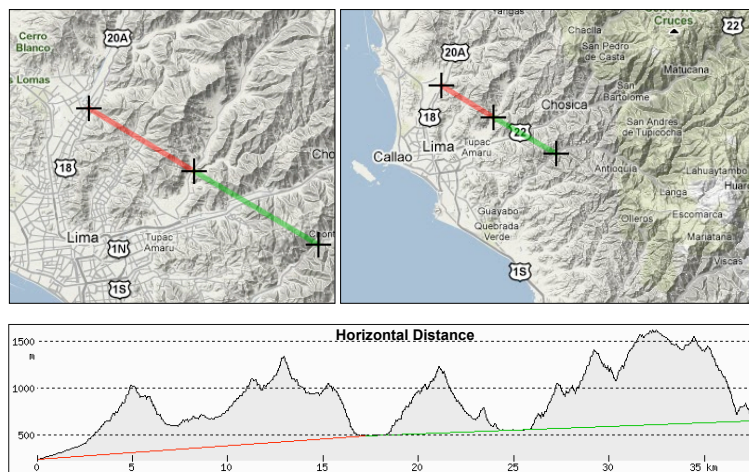


Fig. 1. Top panels show the location and topography surrounding the Jicamarca radar site in Peru, South America. The straight line passing from the northwest to the southeast cuts a height profile as shown in the lower panel, with red indicative of space to the northwest and green indicative of the southeast. The point where the red line and green line meet is the location of Jicamarca. North is towards the top of the page. (Maps from Google Earth, topology from HeyWhatsThat Path Profiler at www.heywhatsthat.com.)

Title Page

Abstract

Introduction

Conclusions

References

Tables

Figures

◀

▶

◀

▶

Back

Close

Full Screen / Esc

Printer-friendly Version

Interactive Discussion



Lower stratospheric doppler ducted gravity waves

Z. Li et al.

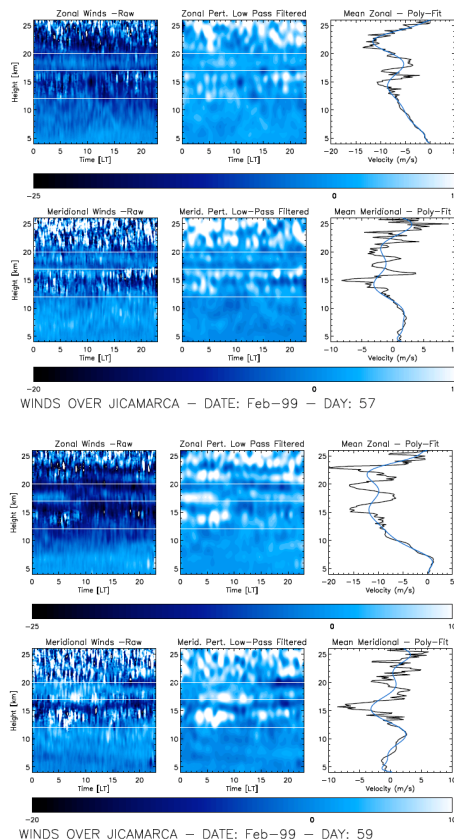


Fig. 2. Contour plots showing MST winds measured over Jicamarca on two days in February 1999. The left column shows the raw zonal (upper row/panel) and meridional (lower row/panel) wind measurements, the right column shows the daily mean winds with a polynomial fit, and the center column shows the low-pass filtered perturbations from the estimated daily mean vertical wind profile. Note that the color scale for the zonal winds is not the same as the color scale for the meridional winds. Horizontal white bars represent bounding heights of high SNR (see text).

Title Page

Abstract

Introduction

Conclusions

References

Tables

Figures

◀

▶

◀

▶

Back

Close

Full Screen / Esc

Printer-friendly Version

Interactive Discussion



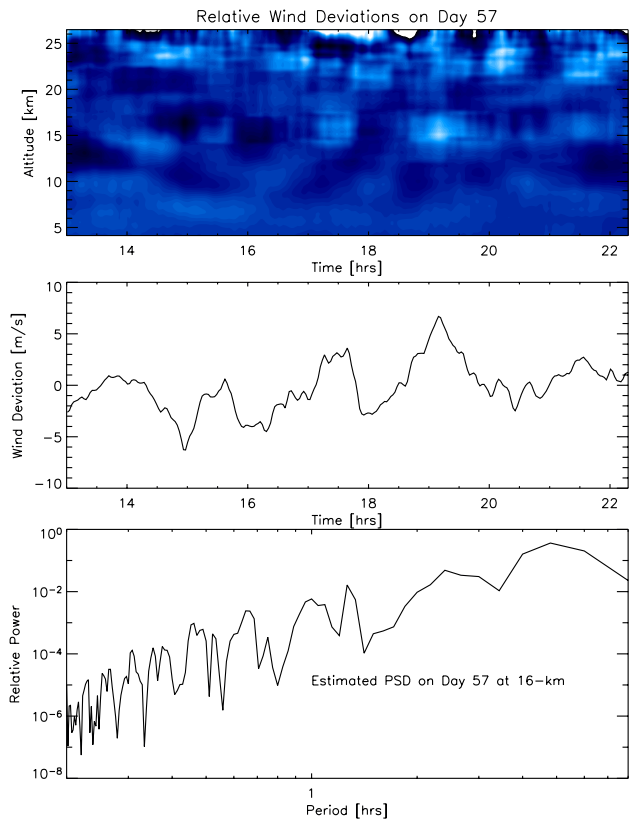


Fig. 3. More detailed view of the ducted feature from day 57. (top) Raw zonal wind deviations from the daily mean wind profile, ranging from -5 m/s to 5 m/s on the black-blue-white color table. No filtering has been utilized. [middle] Wind deviation profile at 16 km. (bottom) An estimate of the power spectral density (PSD) from the 16 km altitude.

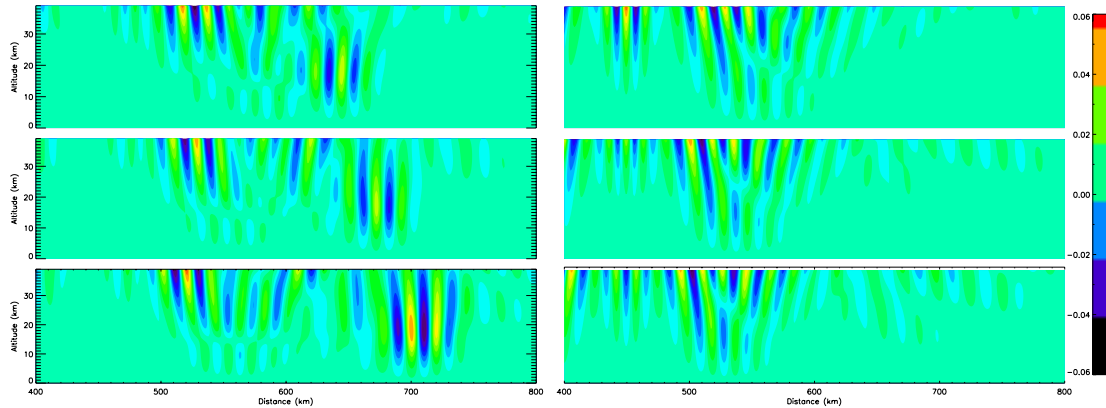


Fig. 4. Vertical velocity simulation results. The left column shows the results of the simulation with a Doppler duct located at ~ 15 km for three progressively increasing time intervals of 12 000 s/3.33 h, 14 000 s/3.89 h, and 16 000 s/4.44 h. The right column shows the results from the simulation without a Doppler duct at the same time intervals. Color-bar units are in m/s.

**Lower stratospheric
doppler ducted
gravity waves**

Z. Li et al.

Title Page

Abstract

Introduction

Conclusions

References

Tables

Figures



Back

Close

Full Screen / Esc

Printer-friendly Version

Interactive Discussion

